

# Ion Transport through Nanoscale Polymer Membranes by Fluorescence Quenching Investigations of CdSe/CdS Quantum Dot/Quantum Rods

Jan-Philip Merkl,<sup>†</sup> Christopher Wolter,<sup>†</sup> Sandra Flessau,<sup>†</sup> Christian Schmidtke,<sup>†</sup> Johannes Ostermann,<sup>†,‡</sup> Artur Feld,<sup>†</sup> Alf Mews<sup>†,‡</sup> and Horst Weller<sup>†,‡,&</sup>

<sup>†</sup> Institute of Physical Chemistry, Grindelallee 117, 20146 Hamburg, and the Hamburg Center for Ultrafast Imaging, University of Hamburg, Luruper Chaussee 149, 22761 Hamburg, Germany, email correspondig author: [weller@chemie.uni-hamburg.de](mailto:weller@chemie.uni-hamburg.de)

<sup>‡</sup> CAN, Center for Applied Nanotechnology, Grindelallee 117, 20146 Hamburg, Germany.

<sup>&</sup> Department of Chemistry, Faculty of Science, King Abdulaziz University, P.O BOX 80203 Jeddah 21589 (Saudi Arabia).

KEYWORDS Fluorescence quenching, single particle investigation, quantum dot in quantum rods, emulsion polymerization, crosslinking, nanochemistry.

## Contents

Experimental section.....	3
Chemicals.....	3
Synthesis of QDQRs and PI- <i>b</i> -PEO Polymers.....	3
Encapsulation of QDQRs, additional chemical reactions and purification .....	3
The use of two different PI- <i>b</i> -PEOs for phase transfer.....	4
The use of different excesses of PI- <i>b</i> -PEO for phase transfer .....	4
Radically initiated cross-linking with AIBN .....	4
Characterization of QDQRs after phase transfer and chemical reactions .....	5
Encapsulation of QDs and purification.....	6
Fluorescence quenching assays of QDQRs encapsulated with two different PI- <i>b</i> -PEO .....	7
Fluorescence quenching assays on single particle scale.....	7
Instrumentation .....	8
Data acquisition and treatment.....	8
Smoluchowski equation.....	9
Results.....	10
Widefield imaging of QDQRs .....	10
Confocal Microscopy .....	10
Control of chemical reaction and long term stability assessment .....	12
Different excesses of PI- <i>b</i> -PEO used for phase transfer of QDQR.....	13
Different cross-linking reactions times using AIBN as cross-linking agent .....	13
Different cross-linking reactions times using PS/DVB as cross-linking agent.....	14
References .....	16

## **Experimental section and particle characterization**

### **Chemicals**

All chemicals were used as purchased, if not stated otherwise. Air or water sensitive chemicals were handled under inert conditions. *n*-Trioctylphosphine (97 %) and *n*-trioctylphosphine oxide (99 %) were purchased from ABCR. Hexylphosphonic acid (100 %) and octadecylphosphonic acid (100 %) were purchased from *PCI Synthesis*. Cadmium oxide (99.998 %, Puratronic®) and copper(II) acetate were purchased from Alfa Aesar. Sulfur (99.998 %), selenium powder (99.99 %), chloroform (anhydrous, amylene stabilized), dichloromethane (anhydrous, amylene stabilized), 1,1'-carbonyldiimidazole (CDI), sodium ascorbate, copper(II) sulfate (98%), *n*-BuLi (1.6 M in *n*-hexane), 2,2'-azobis(2-methylpropionitrile) (AIBN), *s*-BuLi (1.4 M in cyclohexane), PEO300, were purchased from Sigma Aldrich. Azo-bis-(isobutyronitril) (98 %), styrene and divinylbenzene were purchased from Merck. Styrene and divinylbenzene were freshly distilled before usage. Acetone (100 %), chloroform (99 %), ethanol (absolute, undenaturated), *n*-hexane (98.2 %), methanol (100 %), 1-propanol (99 %), sodium hydroxide ENSURE® (Merck Millipore), toluene (100 %), tetrahydrofuran (99.7 % without stabilizers) were purchased from VWR. 2,2'-azobis[2-(2-imidazolin-2-yl)propane]dihydrochloride (VA044) was purchased from Wako Chemicals. Hydrochloric acid (37 %), acetone and tetrahydrofuran (THF) were purchased from Grüssing. Copper acetate (99 %) was purchased from Fluka. Water was purified using a Milli-Q system from Millipore (18,22 MΩ cm).

### **Synthesis of QDQRs and PI-*b*-PEO Polymers**

CdSe/CdS-QDQRs were synthesized by a lightly modified<sup>1,2</sup> procedure reported by Carbone *et al.*<sup>3</sup> and the PI-*b*-PEO polymers were synthesized as described in reference 4. The relative proportion of poly(isoprene) and poly(ethylene oxide) block were 1:2, which is optimal for the formation of spherical micelles. The synthesis of PI was done using *s*-buthyllithium and THF, which is known to yield a PI distribution of approx. 60% 3,4-PI, 30% 1,2-PI and 10% *trans*-1,4-PI.<sup>5</sup> The aspect ratio of QDQRs was 8.4 and a TEM image can be found in Figure ESI 1.

### **Encapsulation of QDQRs, additional chemical reactions and purification**

#### **Encapsulation of QDQRs in PI-*b*-PEO micelles**

The encapsulation was proceeded following a similar procedure reported before by us.<sup>2</sup> Briefly, a ligand exchange with 2,2'-diaminodiethylamine-*block*-polyisoprene (PI-DETA,  $M_w = 1300$  g/mol) was carried out (3500 fold excess of PI-DETA in relation to the QDQRs) over night, before the PI-DETA coated QDQRs were mixed with the poly(isoprene)-*block*-poly(ethylene glycol) (PI-*b*-PEO) PI-*b*-PEO (**1**:  $M_n = 4.3$  kDa,  $M_w = 4.6$  kDa  $M\%(PEO) \sim 68\%$  by NMR, **2**:  $M_n = 13.6$  kDa,  $M_w = 14.3$  kDa  $M\%(PEO) \sim 70\%$  by NMR) in *n*-hexane, dried in nitrogen flow and redispersed in THF and mixed with AIBN in THF (AIBN was added in a 1/3 mass ratio to the used

diblock copolymer). After syringe filtration (Carl Roth, PTFE, 200 nm), the QDQRs/polymer/AIBN were injected into the aqueous phase employing a programmable flow system. The flow system is equipped with a microfluidic reactor chip enabling highly reproducible PI-*b*-PEO-encapsulation and is described in more detail in references <sup>6</sup> and <sup>7</sup>. The purification was carried out using membrane filters (Amicon Ultra MWCO 100 kDa, 3x 15 mL distilled water) and subsequent sucrose density gradient centrifugation. Excess sucrose was removed using membrane filters. A detailed can be found below in the respective paragraph.

#### **The use of two different PI-*b*-PEOs for phase transfer**

To test the influence of two different PI-*b*-PEOs on the properties and the shielding of the QDQRs PI-*b*-PEO **1** of 4.3 kDa and PI-*b*-PEO **2** of 13.6 kDa molecular weight ( $M_w$ ) were used for phase transfer. The above mentioned procedure was used, however 1/3 of AIBN molecules with respect to each PI double bound, were used for cross-linking. The PI-*b*-PEO/QDQR ratio was 1800:1. The cross-linking time was 4 h at 80 °C and purification was carried out as described above. The characterization can be found in the main text.

#### **The use of different excesses of PI-*b*-PEO for phase transfer**

To study the influence of different excesses of PI-*b*-PEO during phase transfer on the density of the polymer shell, the PI-*b*-PEO **2** (13.6 kDa) was used and the excess of PI-*b*-PEO:QDQR was varied between 300:1 and 6000:1. In accordance to our recently published study, we observed QDQR clustering when the PI-*b*-PEO excess was smaller than 1800 PI-*b*-PEO **2**/QDQR.<sup>1,2,6</sup>

#### **Encapsulation of QDQRs via emulsion polymerization**

For the emulsion polymerization 28.5 nmol of QDQRs were used. First the ligand exchange with PI-DETA and the PI-*b*-PEO polymer addition was performed, as described above, however no AIBN was used. The PI-DETA coated QDQRs/PI-*b*-PEO solution in THF was filtered through a PTFE (0.2 μm) syringe filter. The phase transfer to water was performed via the microfluidic reactor chip. The distilled water was flushed with nitrogen for 30 min prior to use. The THF and oxygen were removed by nitrogen flux at 60 °C for 30 minutes. After that small quantities of the radical initiator VA044 (2,2'-azobis[2-(2-imidazolin-2-yl)propane]dihydrochloride) was added and stirred for 15 min at 60 °C. Then 120 μL of 1-pentanol, 100 μL distilled styrene and 100 μL distilled 1,4-divinylbenzene (DVB) were added under vigorous stirring. Samples were taken at 5, 15, 30 min and at 1, 2, 4, 10 h. The polymerization was quenched by adding oxygen saturated water and stirring for 2 min. The taken samples were purified by sucrose density gradient centrifugation. The characterization of the particles can be found in Figure ESI 4.

#### **Radically initiated cross-linking with AIBN**

To study the influence of the reaction time of the cross-linking between the PI moieties (using AIBN as a cross-linking agent), PI-*b*-PEO **2** (13.6 kDa) was used and the ratio between PI-*b*-PEO and QDQR was kept constant at 1800:1. The phase transfer was carried out as described above and 1/3 of AIBN molecules with respect to each PI double bound were added. The cross-linking temperature was 80 °C and the cross-linking time was varied between 0.5 and 10 h. The purification was carried out using sucrose density centrifugation flowed by membrane filtration to remove excess sucrose. The characterization of the particles can be found in Figure ESI 3.

### Characterization of QDQRs after phase transfer and chemical reactions

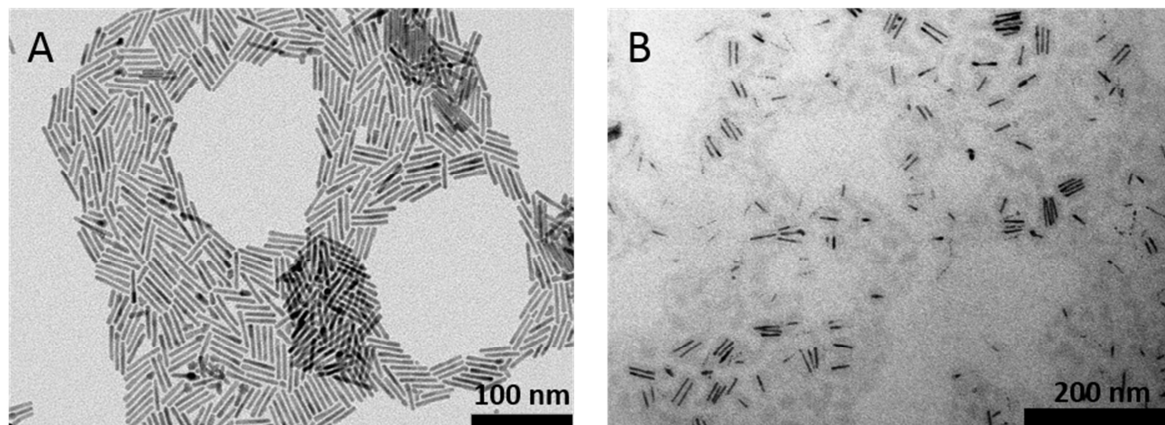


Figure ESI 1: TEM image of the native QDQRs (A, scale bar 100 nm) and QDQRs encapsulated with a PI-*b*-PEO excess of 1800:1 without the addition of AIBN (B, scale bar 200 nm). More detailed TEM investigation is given in references 1 and 2.

The intensity weighed size distribution of the encapsulated QDQRs is shown in Figure ESI 2. The maxima exhibit difference of 10 nm. This is in contrast to the encapsulation of spherical QDs ( $d_{\text{TEM}} \sim 5$  nm), where a more profound difference was detected, using similar PI-*b*-PEOs for phase transfer.<sup>4</sup> This may be due to the bigger size of the QDQRs, which results in different scattering properties of the PI-*b*-PEO-QDQR construct.

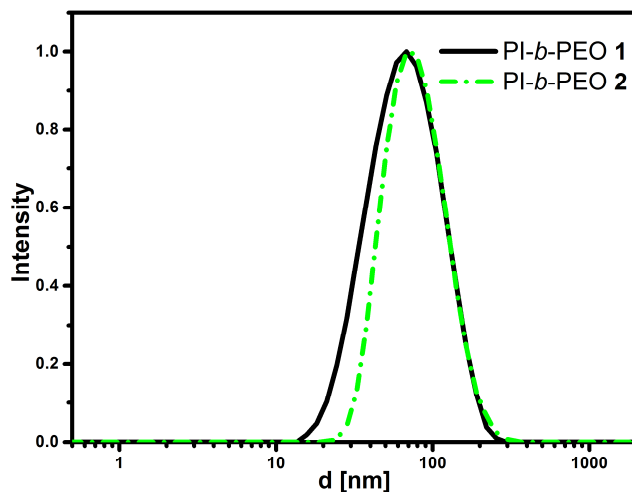


Figure ESI 2: DLS intensity weighed size distribution of QDQRs encapsulated with PI-*b*-PEO 1 and PI-*b*-PEO 2 after 4 h crosslinking reactions with maxima at 68 nm (1) and 78 nm (2).

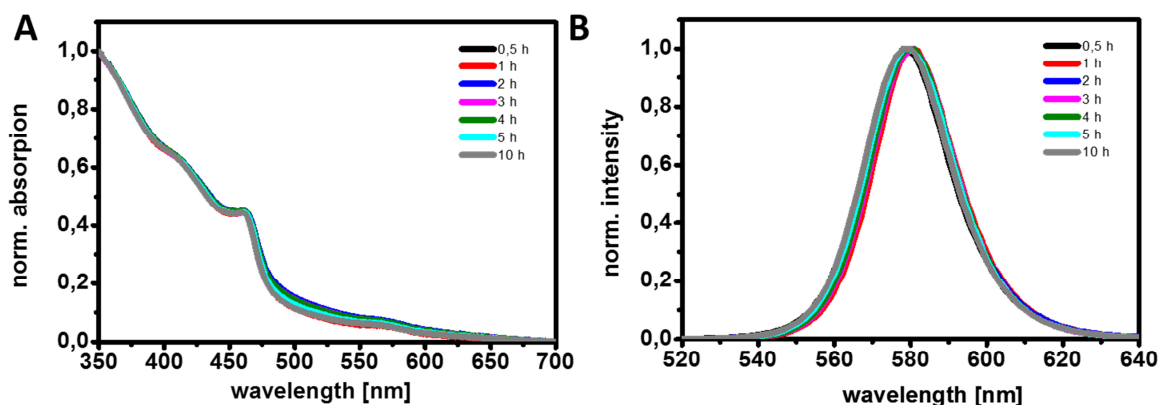


Figure SI 3: Normalized absorption (A) and normalized emission (B) properties of the encapsulated QDQRs during the radical initiated cross-linking reaction using AIBN as initiator. The reaction times are color coded. Figure adapted from reference <sup>8</sup>.

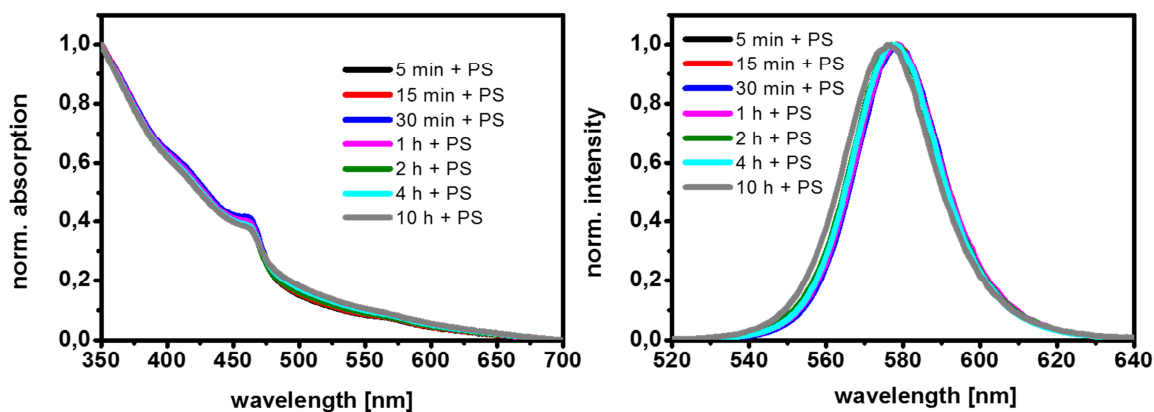


Figure SI 4: Normalized absorption (A) and normalized emission (B) properties of the encapsulated QDQRs during the emulsion polymerization. The reaction times are color coded. Figure adapted from reference <sup>8</sup>.

### Encapsulation of spherical QDs

As a comparison, spherical CdSe/CdS/ZnS were used and transferred as described in detail in reference 4. A ligand exchange with 2,2'-diaminodiethylamine-*block*-polyisoprene (PI-DETA,  $M_w = 1300$  g/mol QD:PI-DETA 1:400) was carried out before the PI-DETA coated QDQRs were mixed with the PI-*b*-PEO **2** in chloroform, dried in nitrogen flow and redispersed in THF. After syringe filtration (0.2  $\mu$ m), the QDQRs were injected into the aqueous phase using the flow device and 1/3 of AIBN molecules with respect to each PI double bound. Here a 4 h cross-linking time was used, as it was found to be optimal with respect to the fluorescence of the QDs.<sup>9</sup> A ligand excess of 400 PI-*b*-PEOs/QD was used which ensures very efficient shielding of QDs.<sup>9,10</sup>

### **Fluorescence quenching assays of QDQRs encapsulated with two different PI-*b*-PEO**

*This assay applies for Figure 1 in the main text.* The QDQRs (100 nM) which were encapsulated with the two different PI-*b*-PEOs were diluted in water or injected into PEG<sub>300</sub> inside a quartz cuvette and equilibrated for 15 min. Absorption, steady-state fluorescence and fluorescence decay spectra (TRSPC) were collected. Aliquots of the copper acetate solution (1.452 mM) were added and kept for 30 min in the dark before absorption, steady-state and fluorescence decay spectra were collected.

### **Fluorescence quenching assays on single particle scale**

The QDQR solution was diluted and applied on a glass cover slide by spin coating so that single nanoparticles lay separately from each other. The glass cover was fixed in a liquid cell where polyethylene glycol PEO300 (Sigma Aldrich) and subsequently a PEO300- copper(II) acetate solution was added and mixed with the pipette. The final concentration of the copper(II) acetate solution was varied with an upper level of 4 mM. Single particles were identified by their half width at half maximum value: Before the PL quenching experiment, a PL spectra of the confocal spot was measured and analyzed. If the half width at half maximum value of the PL spectrum was larger than 22 nm, the data were not included in the analysis for single particle investigations. The same applied when the spectra showed multiple maxima.<sup>11</sup> We investigated the PL decay as well as the PL intensity time trace for at least 5 min.

### **Long term accessibility tests and fluorescence quenching assays**

*This assay applies for the long term accessibility tests (Figure 3 and Figures ESI 8-11).* To test the long term stability of the fluorescence of the encapsulated QDQRs against Cu<sup>2+</sup> ions (as a test of the density of the polymer shell) a 100 nM aqueous solution of the encapsulated QDQRs in a quartz cuvette was mixed with 800 eq. of Cu(II)acetate. The fluorescence intensity of the QDQRs was measured before the addition of the Cu<sup>2+</sup> ions and then the change of the fluorescence intensity after Cu<sup>2+</sup> ions was followed for 7 days. The respective time points for the PL-intensity determination were: 1 s, 10 s, 20 s, 1, 2, 3, 4, 5, 6, 7, 10, 20, 30 min, 1 h, 2 h, 3 h, 5 h, 1 d, 2 d, 3 d, 4 d, 5 d, 6 d, 7d.

The assessment of the density of the polymer shell against pH values ranging from 3-11 were conducted in a comparable manner by measuring the PL-intensity of the encapsulated QDQRs over time. First, 1 mL of aqueous solution of the pH 3 or 5, 7, 9, 11 in a cuvette was mixed with a small volume of QDQRs so that the final concentration of encapsulated QDQRs in the cuvette was 100 nM. The PL-intensity was normalized to the PL-Intensity at pH 7 at t= 0 s.

## Instrumentation

Absorption measurements were made with a Cary 50 from Varian and steady-state fluorescence was measured using a Fluoromax 4 from Horiba Jobin Yvon. The fluorescence decay was measured using an excitation wavelength  $\lambda = 438$  nm from a PDL 800-D pulsed diode laser and with a PMA-M185 photomultiplier with a resolution of 500 ps (PicoQuant). The signal was processed by a constant fraction 200 MHz discriminator and a time-to-amplitude converter (EG&G Ortec). Fluorescence decay curves were fitted with a stretched mono-exponential (equation SI 1) and the average lifetime were calculated using the gamma function (equation SI 2).

For wide-field imaging, a CW power of typically 186  $\mu$ W was used, measured in front of the objective with a power meter. For single particle investigation the expanded beam of a 485 nm pulsed diode laser (PDL 800-D, LDH-D-C-485, PicoQuant GmbH) with a power of 1.3  $\mu$ W illuminated the sample. Neutral density filters were used to adjust the excitation beam to a suitable intensity (14 nW).<sup>1</sup> The emission from the nanoparticle was collected by a 100x magnification oil objective with a numerical aperture of 1.25 (Zeiss Achroplan), separated from the scattered laser light by a longpass filter with 522 nm edge wavelength (FF01-515/LP-25, Semrock), and focused with the help of an additional lens to a charge coupled device (CCD) camera (ProEM 512B, Princeton Instruments) for widefield images.

## Data acquisition and treatment

The analysis of the fluorescence decay time in dependence of the quencher concentration was preceded using a stretched mono-exponential decay (equation ESI 1).  $FI(t)$  is the time dependent fluorescence and  $A(Q)$  is the pre-exponential factor and expresses the signal height, which may be used to quantify the static quenching.<sup>4</sup> The stretching exponent  $\beta$  is a measure of relaxation rates in the fluorescence decay, and  $\tau_i$  exhibits the fluorescence lifetime.<sup>12</sup>

$$FI(t) = A(Q)e^{(t/\tau_i)^\beta} \quad \text{eq. ESI 1}$$

The average fluorescence decay time  $\tau_Q$  was calculated using the gamma function eq. ESI 2.<sup>5</sup>

$$\langle \tau_Q \rangle = \left(\frac{\tau_i}{\beta}\right) \Gamma\left(\frac{1}{\beta}\right) \quad \text{eq. ESI 2}$$

### Smoluchowski equation

To approximate the diffusion of Cu(II) ions inside the PI-membrane a biomolecular rate constant  $k_0$  was extracted from the dynamic quenching rate and the Smoluchowski equation (eq. ESI 3) was used.<sup>13,14</sup>

$$k_0 = 4\pi N_A R_0 (D_{Cu(II)} + D_{QDQR}) \quad \text{eq. SI 3}$$

Here  $D_i$  is the respective diffusion coefficient ( $D_{QDQR}$  set to 0, due to relative movement of Cu(II) towards QDQR),  $N_A$  the Avogadro number and  $R_0$  the tunneling radius of the electron transfer, set to 0.5 nm. Here we assumed, that the measure for the quenching efficiency  $f_Q$  is 1 (equation ESI 4) and that the Stern-Volmer constant  $K_{SV}$  is the product of bimolecular quenching constant and the PL lifetime in absence of a quencher (equation ESI 5).

$$k_q = k_0 f_Q \quad \text{eq. SI 4}$$

$$K_{SV} = k_q \tau_0 \quad \text{eq. SI 5}$$

## Results

### Widefield imaging of QDQRs

The spin coated QDQRs were applied to a liquid chamber and investigated using a widefield microscopy setup.<sup>11</sup> PEO300 was used as a solvent. After the QDQRs were put into focus, Cu(II)acetate in PEO300 was added and mixed with the pipette. Representative widefield images before (A,C) and 30 min after (B,D) the addition of 8  $\mu$ M Cu(II)acetate are shown in Figure ESI 5. The measurement was repeated 4 times and approx.. 80% of the PI-*b*-PEO **1** QDQRs were quenched whereas 40% of the PI-*b*-PEO **2** encapsulated QDQRs were quenched statically.

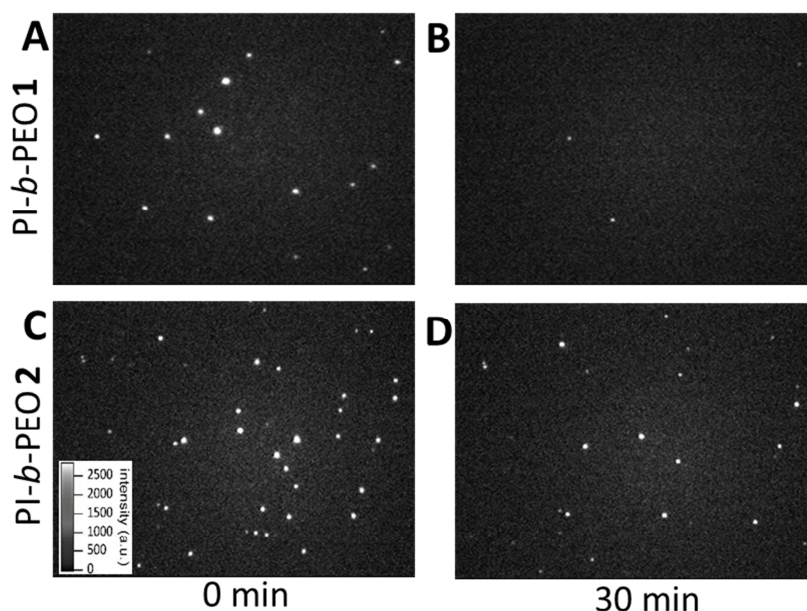


*Figure ESI 5:* Widefield fluorescence image before (A, C) and 30 min after (B, D) the addition of 8  $\mu$ M Cu(II)acetate of differently encapsulated QDQRs (A, B: PI-*b*-PEO **1**, C, D: PI-*b*-PEO **2**). Dimension of the images approx. 30x50  $\mu$ m.

### Confocal Microscopy

The spin coated QDQRs were analyzed using time-resolved confocal microscopy. The confocal setup enables the selective positioning of an individual QDQR in the focused excitation volume and simultaneously the exclusive collection of the emitted fluorescence light of just the same QDQR. Single particles were identified by their PL spectra half width at half maximum (< 22 nm).<sup>1,11</sup>

In Figure ESI 6 representative time traces of two different, single-encapsulated QDQR (A,C) in PEO300 under laser excitation are shown. Due to the low power, QDQRs did not exhibit pronounced fluorescence blinking.<sup>1</sup> After the incubation with copper(II) acetate (approx. 10 min) the PL intensity was reduced, however still detectable and over the background signal level, as already shown from widefield images. When the focused laser beam (14 nW, spot diameter approx. 300 nm) was then moved to a single QDQR, in some particles, an acceleration in PL degradation was observed (Fig. ESI 6 B). This process was significantly accelerated when higher excitation powers (45 nW) were used, which may correlate with a report by *Isarov and Chrysochoos*, where a charge transfer from an exciton to Cu(II) and/or Cu(I) was discussed.<sup>15</sup>

The associated lifetimes are presented in the main text. The histograms were fitted with equation ESI 6, and the extracted parameters can be found in Table ESI 1.

$$y = y_0 + \frac{A}{w\sqrt{2\pi}} \exp\left(-2 \frac{(x-x_c)^2}{w^2}\right) \quad \text{eq. ESI 6}$$

The associated stretching exponent  $\beta$  of single spin coated QDQRs changed when copper(II) acetate was present in solution. After the addition of copper(II) acetate, the QDQRs encapsulated with the small polymer **1** (Figure ESI 7, C) exhibit in average a lower stretching exponent, than QDQRs encapsulated with the bigger polymer **2** (Figure ESI 7, D).

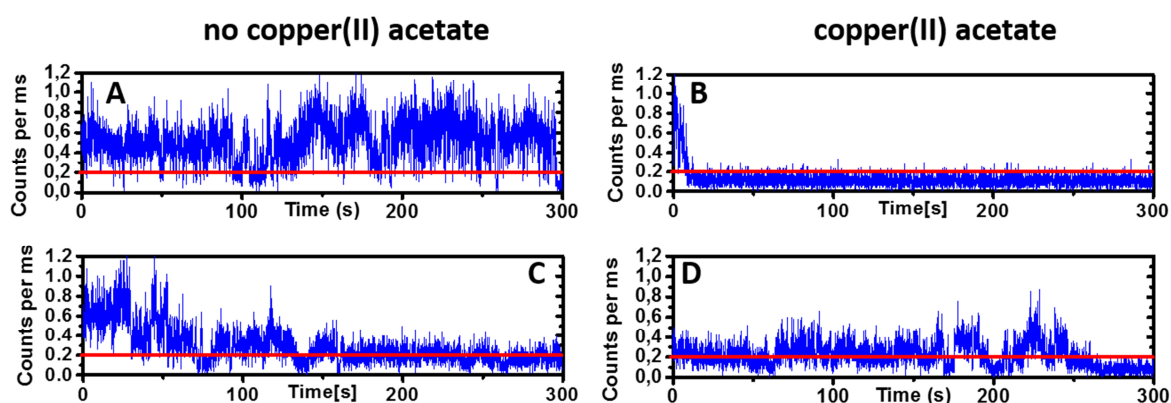


*Figure ESI 6:* Representative time traces of two individual encapsulated QDQRs in PEO300 (top and bottom row). On the left hand side (A,C) the time traces in absence of the copper(II) acetate are shown. On the right hand side the encapsulated QDQRs in the presence of copper(II) acetate are shown. The red line represents the level of background fluorescence under the chosen excitation parameters.

Table ESI 1: Fit Parameters of the Gaussian fit of the fluorescence lifetime histogram of the manuscript using equation ESI 6.

	$y_0$	$x_c [ns]$	$w [ns]$	<b>A</b>
PI- <i>b</i> -PEO 1 <b>No Cu(II)</b>	0.29±0.46	9.8±0.3	5.9±0.9	43.7±8.2
PI- <i>b</i> -PEO 1 <b>c(Cu(II)acetate)=3.9 μM</b>	0.35±0.25	5.2±0.3	4.2±0.5	29.7±4.1
PI- <i>b</i> -PEO 2 <b>No Cu(II)</b>	0.37±1.10	10.5±0.8	6.8±2.2	54.2±22.1
PI- <i>b</i> -PEO 2 <b>c(Cu(II)acetate)=3.9 μM</b>	0.27±0.83	10.7±0.6	6.5±1.4	79.9±18.8

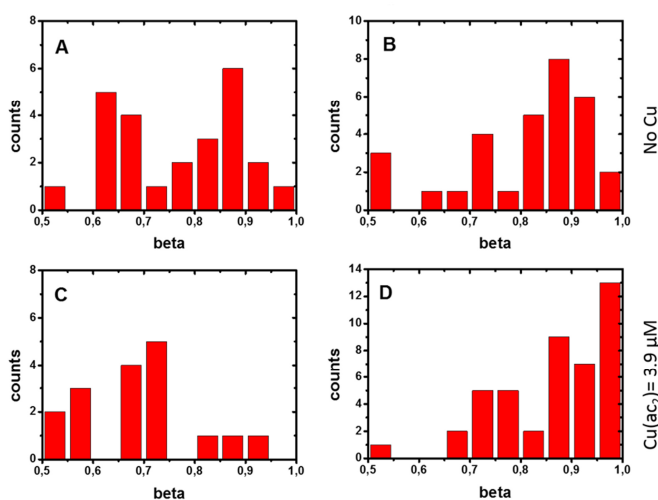


Figure ESI 7: Histogram (binning 0.05) of the stretching exponent  $\beta$  before (A, B) and after (C, D) the addition of copper(II) acetate ( $c= 3.9 \mu\text{M}$ ) to the QDQRs encapsulated with the PI-*b*-PEO 1 (left, A,C) and the PI-*b*-PEO 2 (right B,D).

### Control of chemical reaction and long term stability assessment

In Figure ESI 8 the temporal evolution of the relative PL-intensity after the addition of 800 equivalents of the QDQRs transferred to water with a different excess of PI-*b*-PEO/QDQRs

in different media is presented. The PL of QDQRs without any polymer shell is quenched by the Cu(II) ions immediately and completely, this was tested by dissolving the native QDQRs in *n*-hexane and adding the same amount of Cu(II)acetate as a THF solution (Figure ESI 8 A, black bars). With increasing excess of the PI-*b*-PEO polymer the micelles become more dense against Cu(II) penetration with a maximum at an 1:3500 excess. As a comparison, the relative PL intensity of encapsulated QDs (dark blue) is shown.

In Figure ESI 8 B-F the relative PL intensity of the different QDQR constructs at different pH values (color coded) is shown. The density of the polymer micelles against very acidic to very basic media (pH3-11) increases with increasing excess of polymer used for the encapsulation process. It is obvious, that the shielding of the QDQRs against Cu(II) ions or protons without cross-linking is not optimal.

#### Different excesses of PI-*b*-PEO used for phase transfer of QDQR

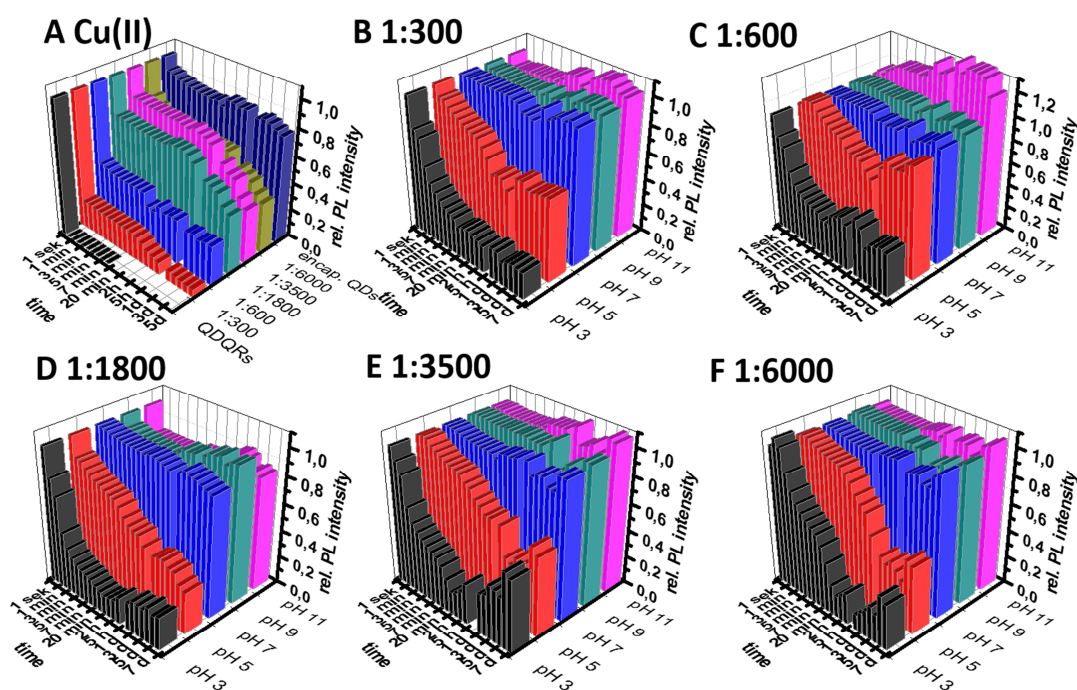
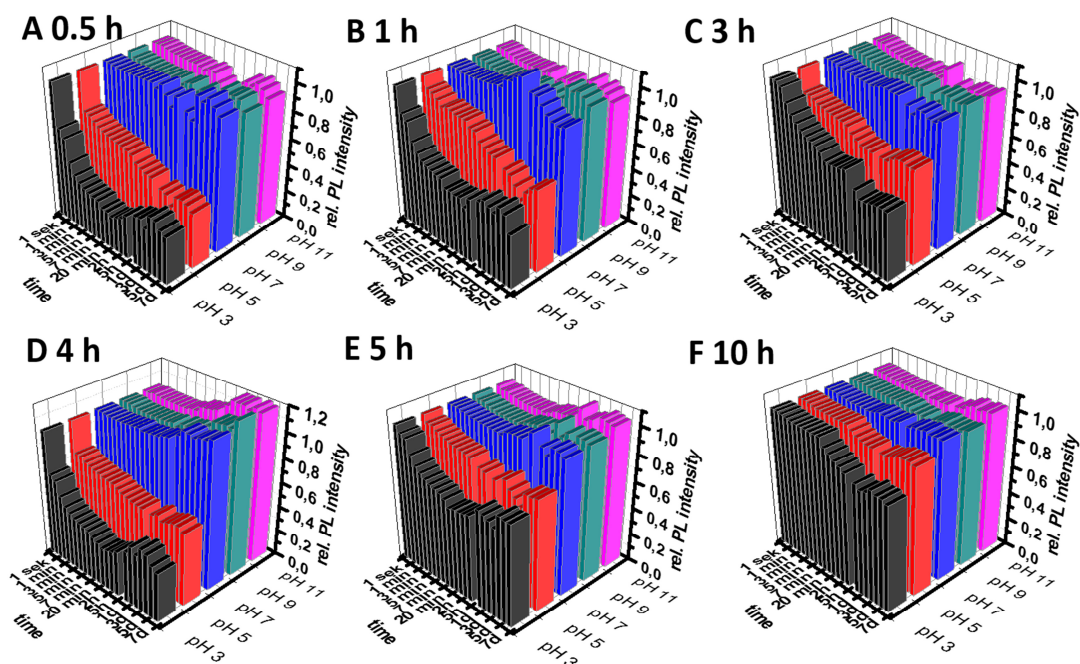


Figure ESI 8: Relative PL-intensity of PI-*b*-PEO 2 encapsulated QDQRs with different excess of polymer (1:300, 1:600, 1:1800, 1:3500, and 1:6000). A) PL-Intensity after addition of 800 eq of Cu(II) and B-F) at pH values between 3 and 11. The PL-intensity was normalized to the respective PL-Intensity at pH 7 at t= 0 s.

#### Different cross-linking reactions times using AIBN as cross-linking agent

In Figure ESI 10 A-F the relative PL intensity of QDQRs at different pH values is presented. An efficient shielding against protons can only be achieved, when long cross-linking reaction times (5-10 h) are used.



**Figure SI 9:** Relative PL-intensity of PI-*b*-PEO **2** encapsulated QDQRs with different cross-linking times (A-F, times mentioned in the description) using AIBN as a cross-linking agent. The PL-intensity is recorded over a period of 7 days after transferring the encapsulated QDQRs into aqueous media at a certain pH value. The different pH values are pH 3: black, pH 5: red, pH 7: blue, pH 9: turquoise, pH 11: purple. The PL-intensity was normalized to the respective PL-Intensity at pH 7 at t= 0 s.

#### Different cross-linking reactions times using PS/DVB as cross-linking agent

In Figure ESI 10 the temporal evolution of the relative PL intensity of encapsulated QDQRs after the addition of 800 equivalents Cu(II) is shown. Here the QDQRs were encapsulated with PI-*b*-PEO **2** and a emulsion polymerization with DVB and styrene of different reactions times was used to shield the particles. Long reaction times are needed to shield the QDQRs efficiently against Cu(II) ions. In Figure ESI 12 A-F the pH-sensitivity of the PL of encapsulated QDQRs is presented. Even short reaction times allow adequate shielding of QDQRs against protons. The styrene shell protects the fluorescent QDQRs from very acidic to very basic pH values and high Cu(II) concentrations.

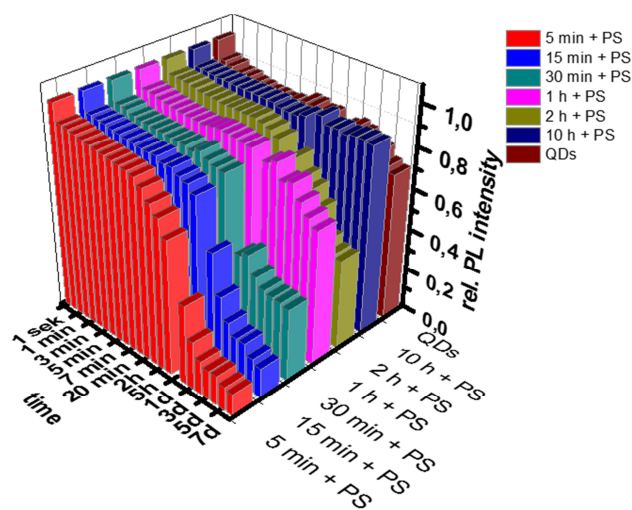


Figure ESI 10: Relative PL-intensity of QDQRs encapsulated via emulsion polymerization (using PI-*b*-PEO **2**, styrene and 1,4-divinylbenzene) after addition of 800 eq of Cu(II) over a period of 7 days. As a comparison, spherical QDs encapsulated in PI-*b*-PEO **2** are shown (without EP).

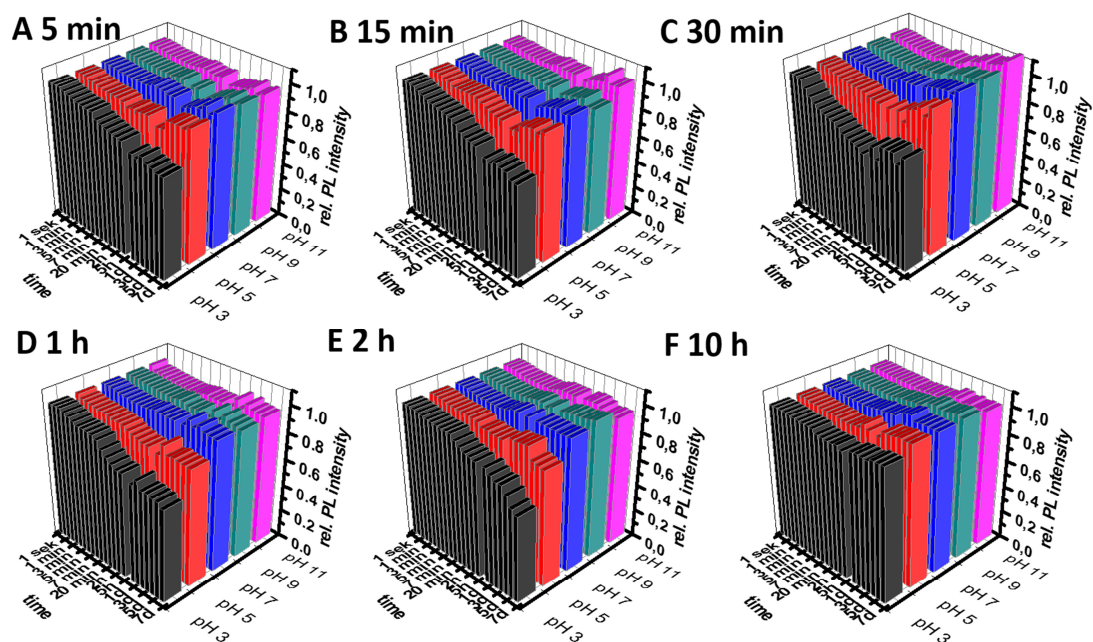


Figure ESI 11: Relative PL-intensity of QDQRs encapsulated via emulsion polymerization (using PI-*b*-PEO **2**, styrene and 1,4-divinylbenzene) in dependence of the reaction time. The different pH values are pH 3: black, pH 5: red, pH 7: blue, pH 9: turquoise, pH 11: purple. The PL-intensity was normalized to the respective PL-Intensity at pH 7 at  $t = 0$  s.

## References

- 1 M. Rafipoor, C. Schmidtke, C. Wolter, C. Strelow, H. Weller and H. Lange, *Langmuir*, 2015, **31**, 9441–9447.
- 2 J. Dimitrijevic, L. Krapf, C. Wolter, C. Schmidtke, J.-P. Merkl, T. Jochum, A. Kornowski, A. Schüth, A. Gebert, G. Hüttmann, T. Vossmeier and H. Weller, *Nanoscale*, 2014, **6**, 10413–22.
- 3 L. Carbone, C. Nobile, M. De Giorgi, F. Della Sala, G. Morello, P. Pompa, M. Hytch, E. Snoeck, A. Fiore, I. R. Franchini, M. Nadasan, A. F. Silvestre, L. Chiodo, S. Kudera, R. Cingolani, R. Krahne and L. Manna, *Nano Lett.*, 2007, **7**, 2942–50.
- 4 J. Ostermann, J.-P. Merkl, S. Flessau, C. Wolter, A. Kornowski, C. Schmidtke, A. Pietsch, H. Kloust, A. Feld and H. Weller, *ACS Nano*, 2013, **7**, 9156–9167.
- 5 M. F. Al-Jarrah, R. Apikian and E. Ahmed, *Polym. Bull.*, 1984, **12**, 433–436.
- 6 C. Schmidtke, R. Eggers, R. Zierold, A. Feld, H. Kloust, C. Wolter, J. Ostermann, J.-P. Merkl, T. Schotten, K. Nielsch and H. Weller, *Langmuir*, 2014, **30**, 11190–11196.
- 7 E. Pösel, C. Schmidtke, S. Fischer, K. Peldschus, J. Salamon, H. Kloust, H. Tran, A. Pietsch, M. Heine, G. Adam, U. Schumacher, C. Wagener, S. Förster and H. Weller, *ACS Nano*, 2012, **6**, 3346–3355.
- 8 C. Wolter, University of Hamburg, 2015.
- 9 C. Schmidtke, H. Lange, H. Tran, J. Ostermann, H. Kloust, N. G. Bastús, J.-P. Merkl, C. Thomsen and H. Weller, *J. Phys. Chem. C*, 2013, **117**, 8570–8578.
- 10 J.-P. Merkl, J. Ostermann, C. Schmidtke, H. Kloust, R. Eggers, A. Feld, C. Wolter, A.-M. Kreuziger, S. Flessau, H. Mattoussi and H. Weller, in *Proc. of SPIE 8955*, eds. W. J. Parak,

- M. Osinski and K. I. Yamamoto, 2014, vol. 8955, p. 89551X.
- 11 S. Flessau, C. Wolter, E. Poselt, E. Kroger, A. Mews and T. Kipp, *Phys. Chem. Chem. Phys.*, 2014, **16**, 10444–10455.
  - 12 G. Schlegel, J. Bohnenberger, I. Potapova and A. Mews, *Phys. Rev. Lett.*, 2002, **88**, 1–4.
  - 13 J. R. Lakowicz, *Principles of Fluorescence Spectroscopy*, Springer Science+Buisness Media, New York, Third Edit., 2006.
  - 14 M. Smoluchowski, *Ann. Phys.*, 1915, **48**, 1103–1112.
  - 15 A. V. Isarov and J. Chrysochoos, *Langmuir*, 1997, **13**, 3142–3149.